ISSN 1330-3651 (Print), ISSN 1848-6339 (Online)
DOI: 10.17559/TV-20151027082900

EVOLUTION CHARACTERISTICS ANALYSIS OF PRESSURE-ARCH IN A DOUBLE-ARCH TUNNEL

Shu-ren Wang, Chun-liu Li, Yong-guang Wang, Zheng-sheng Zou

Original scientific paper

In order to provide a basis for the reinforcement design and construction safety of the double-arch tunnel, it is of theoretical and practical value to analyse the morphological characterization, the evolution process and the skewed effect of the pressure-arch in a double-arch tunnel. Based on the descriptions of the boundary parameters of the pressure-arch in a double-arch tunnel, taking the 80 m buried depth double-arch highway tunnel as the research object, the numerical calculation model of the double-arch tunnel was built by using FLAC3D, and then the morphological evolution of the pressure-arch induced by step-by-step excavation was analysed. The results showed that the pressure-arch of the double-arch tunnel displayed the skewed distribution characteristics which were gradually diminishing from the left tunnel to the right tunnel, the strain energy dissipation of the double-arch tunnel from the left tunnel to the right tunnel was from high to low, and the nonlinear response characteristics in different excavation sequences were sensitive to the changes of the stress state. The results provided a basis for the rock reinforcement design and safety construction of double-arch tunnel.

Keywords: *double-arch tunnel; numerical calculation; pressure-arch; skewed effect; strain energy*

Analiza razvoja značajki tlačnog svoda u tunelu s dvostrukim svodom

Izvorni znanstveni članak

Kako bi se osigurala osnova za pojačanje konstrukcije i sigurnost izgradnje tunela s dvostrukim svodom, od teorijske i praktične vrijednosti je analizirati morfološku karakterizaciju, proces razvoja i asimetrični učinak tlačnog svoda u tunelu s dvostrukim svodom. Na temelju opisa graničnih parametara tlačnog svoda u tunelu s dvostrukim svodom, kao istraživački objekt uzet je tunel autoceste s dvostrukim svodom iskopan na dubini od 80 m, te je izrađen numerički proračunski model tunela s dvostrukim svodom uporabom FLAC3D, a potom je analiziran morfološki razvoj tlačnog svoda induciran iskopom korak-po-korak. Rezultati su pokazali da tlačni svod tunela s dvostrukim svodom pokazuje karakteristike asimetrične distribucije koja se postupno smanjuje od lijevog tunela ka desnom tunelu, da rasipanje energije deformacije tunela s dvostrukim svodom od lijevog tunela ka desnom tunelu ide od visokog do niskog, te da su nelinearne odzivne karakteristike u različitim sekvencama iskopa osjetljive na promjene u stanju naprezanja. Rezultatima je omogućena osnova za konstrukcije pojačane kamenom i sigurnost u izgradnji tunela s dvostrukim svodom.

Ključne riječi: *asimetrični učinak; energija deformacije; numerički proračun; tlačni svod; tunel s dvostrukim svodom*

1 Introduction

The double-arch tunnel is a special tunnel and its lining structures between two adjacent tunnels are supported by the pillar between them. Owing to the large span and large rock pressure, the two single tunnels of the double-arch tunnel excavated interfere mutually that makes the supporting system become much complicated, let alone in the weak surrounding rock with frequent collapse or roof caving accident [1, 2]. Thus, the evolution process and the skewed effect (The geometry and deformation parameters of the pressure-arch are not symmetrical after the double-arch tunnel being excavated, we called these characteristics the skewed effect) of the pressure-arch under the step-by-step excavation are essential problems, which have been of wide concern for the scholars and technical personnel in the field of engineering.

In the past years, the skewed pressure problems under the tunnel construction have been analysed by many scholars. For example, Kovari first found there was a pressure-arch effect in the loose rock with the tunnel excavation [3]. Protodyakonov proposed the collapsing arch theory of the loose rock [4]. Terzaghi proposed the existence conditions of the pressure-arch of the excavated sand chamber by the experiment [5]. Rabcewicz proposed that a self-bearing structure could form in the surrounding rock of the chamber in New Austrian Tunnelling Method [6]. Huang et al. proposed the identification method of the upper and lower boundaries of the pressure-arch [7]. Poulsen conducted the Coal pillar load calculation by pressure arch theory [8]. Fraldi et al. provided an idea to analyse instability problems of the tunnel [9]. The Chinese scholars such as Li et al. monitored the construction deformation of the large span multi-arch tunnel under complex geological conditions, and proposed the engineering measures to control the large deformation [10]. Zhu et al. analysed the construction sequence and the supporting force of the shallow-buried tunnel by numerical simulation method [11]. Combining physical model experiment with numerical simulation, Jin et al. analysed the temporal-spatial effect of the force and deformation of the supporting structure of the six-lane multi-arch tunnel [12]. Based on the monitoring data and numerical model, Monjezi et al. analysed the instability and ground subsidence characteristics of a shallow depth metro tunnel [13]. Yang et al. analysed the stability of the pressure arch and the instability failure modes after the tunnel excavation using similar model test, [14]. Chen et al. analysed the stress redistribution and ground arch development during the tunnel construction [15], and so on.

In summary, there are rich achievements in the world on the research of pressure-arch in the double-arch tunnel, but there are still some questions not being solved well. Thus taking the double-arch tunnel as an example, the evolution mechanism and the skewed effect of the pressure-arch during step-by-step excavation need to be further studied.

2 Pressure-arch shape-parameters of double-arch tunnel

In order to facilitate the study, the element stress variable e was defined [14]

$$e = \frac{\sigma_{\max} - \sigma_{\min}}{\sigma_{\max}} \times 100\,\%, \quad (1)$$

where $\sigma_{\max}$ and $\sigma_{\min}$ were maximum and minimum principal stress of the surrounding rock unit respectively after the double-arch tunnel was excavated.

As shown in Fig. 1, corresponding to the peak point A of the maximum principal stress of the surrounding rock, the boundary was defined as the inner boundary of the pressure-arch. When the stress variable e was equal to 10 %, the boundary corresponding to point B was defined as the outer boundary of the pressure-arch. On both lateral walls corner of the double-arch tunnel, extending toward the deep of the surrounding rock and meeting with the inner and outer boundaries of the pressure-arch along the rock rupture angle β, the closed region was the pressure-arch area. According to the Protodyakonov's theory and Rankine theory, the rock rupture angle is $\beta = 45° + \varphi/2$, where φ was the inner friction angle of the surrounding rock of the double-arch tunnel.

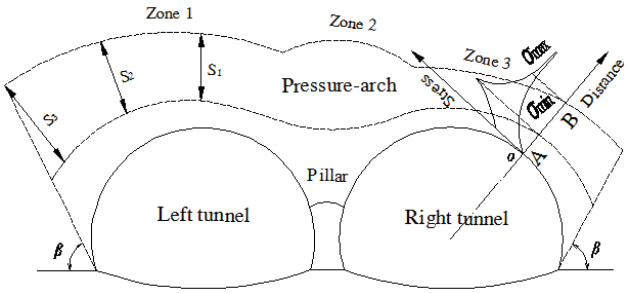

Figure 1 Pressure-arch zones and morphological parameters of the double-arch tunnel

As shown in Fig. 1, the pressure-arch of the double-arch tunnel was divided into three zones so as to simplify the analysis. For Zone 1, the characteristic parameters of the pressure-arch were defined as the vault thickness S_1, the waist thickness S_2 and the skewback thickness S_3 of the pressure-arch, respectively. It is the same with Zone 2 and Zone 3.

The mechanics and engineering significance of the pressure-arch of the double-arch tunnel are as follows: during step-by-step excavation of the double-arch tunnel, the surrounding rock experienced stress redistribution repeatedly, and a skewed complex self-bearing pressure-arch finally formed near the excavation area of the double-arch tunnel. The morphological characteristics of the pressure-arch and the arch thickness in separate zones could demonstrate the disturbance effect of the surrounding rock. Much more, the studies on the mechanical evolution process and the skewed characteristic of the pressure-arch provided a basis for supporting design and construction safety of the double-arch tunnel.

3 Computational model and simulation analysis schemes

3.1 The computational model

The shape and dimension of the designed cross-section of the double-arch tunnel are shown in Fig. 2a. The tunnel with 80 m burial depth was excavated by the bench method, and its surrounding rock was mainly composed of medium weathered sandstone, while the hydro-geological conditions were simple.

Since there were some difficulties in modeling and meshing for complicated 3D engineering in FLAC3D, firstly, we built the engineering-geological model using ANSYS, and then the engineering-geological model was imported into FLAC3D as shown in Fig. 2b. According to the sizes in Fig. 2a, the dimensions of the model were 70 m long, 4 m wide and 40 m high in the *x*-, *y*-, and *z*- axis, separately. The model was divided into 9536 elements. Since the infinite long tunnel can be treated as a plane problem (the axial length of the model 4 m was thin comparing with the 70 m length and the 40 m height of the model) through the simplified method, therefore, the axial length of the model was thin. The horizontal displacements of four lateral boundaries of the model were restricted, and its bottom was fixed. The upper surface of model was the load boundary, and on it the vertical load converted from the weight of the overlying rock mass was applied. The material of model was supposed to meet the Mohr-Coulomb strength criterion, and moreover, it was supposed that the model was in the hydrostatic stress state, namely the lateral pressure coefficient λ was 1,0. The parameters were selected as listed in Tab. 1.

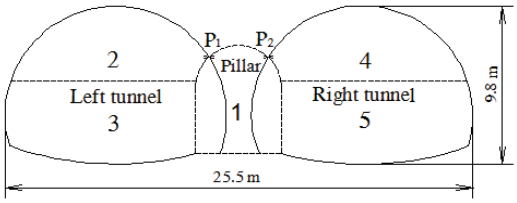

a) Excavation steps of the tunnel

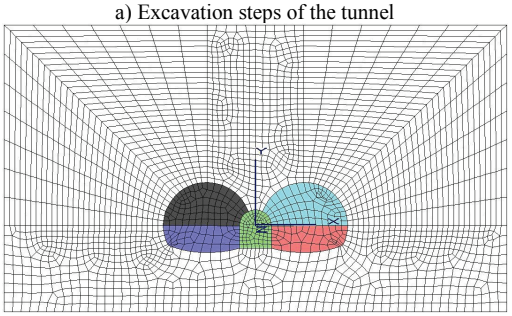

b) Computational model and its meshing

Figure 2 Excavation steps of the tunnel and the computational model

Table 1 Physical and mechanical parameters of the surrounding rock of the double-arch tunnel

Density (kg/m^3)	Elasticity modulus (GPa)	Poisson ratio	Tensile strength (MPa)	Cohesion (MPa)	Friction angle (°)
2500	20,0	0,30	0,5	1,5	48

3.2 Simulation analysis schemes

The double-arch tunnel was excavated by the bench method to analyse the evolution characteristics of the

pressure-arch. The bench method construction was divided into five steps, and the construction sequence is shown in Fig. 2a:

Step 1: After the initial stress field of the calculation model was balanced, the displacement and the velocity field were cleared and then the pilot tunnel 1 was excavated.

Step 2: After reconstructing the pillar with concrete material to improve the strength of the pillar, the upper cross-section 2 of the left tunnel was excavated.

Step 3: The lower cross section 3 of the left tunnel was excavated.

Step 4: The upper cross section 4 of the right tunnel was excavated.

Step 5: The lower cross section 5 of the right tunnel was excavated.

Based on the above numerical simulation, the pressure-arch shape and evolution process of the pressure-arch could be revealed. Then by defining the skewed coefficient and introducing the concept of strain energy entropy, the skewed effect and the strain energy dissipation characteristics of surrounding rock of the double-arch tunnel were analysed (Fig. 3e).

3.3 Evolution characteristics analysis of the pressure-arch under different conditions

(1) Geometric size effect

In order to reveal the size effect of the pressure-arch, the evolution characteristics of the pressure-arch of two-lane and three-lane tunnels during step-by-step excavation were compared and analysed.

(2) Excavation sequence effect

The excavation sequence of bench method and expanding method were 1-2-3-4-5 and 1-2-4-3-5, respectively. The comparative analysis of evolution characteristics of the pressure-arch under two different sequences could reveal the nonlinear response characteristics with the different excavation sequence.

(3) Stress state effect

Considering the impact of the lateral pressure, three kinds of stress state were used. The comparative analysis of evolution characteristics of the pressure-arch in double-arch tunnel under different stress states could reveal the skewed effects of the pressure-arch.

4 Evolution character of pressure-arch in the double-arch tunnel during step-by-step excavation

4.1 Evolution process and morphological character of the pressure-arch

The evolution process analysis of the pressure-arch in double-arch tunnel under bench excavation method was conducted as the following.

Step 1: As shown in Fig. 3a, after the middle pilot tunnel being excavated, due to the stress self-adjusting effect of the surrounding rock, a symmetrical pressure-arch zone 2 gradually formed at the top of the middle pilot (The white dotted lines on both sides of the middle pilot tunnel were the side boundaries of the pressure-arch, and the white dotted curve boundary close to the excavation face was its inner boundary, and its outer boundary was the graphic outer contour.).

Step 2: As shown in Fig. 3b, after the pillar being reconstructed, the upper cross-section 2 of the left tunnel was excavated, zone 1 of the pressure-arch on the top of the left tunnel was formed, zone 2 of the pressure-arch offset to the right obviously, and the pressure-arch thickness increased. There was an obvious boundary between zone 1 and zone 2 of the pressure-arch. The pressure distribution in the top of the pillar was not symmetrical.

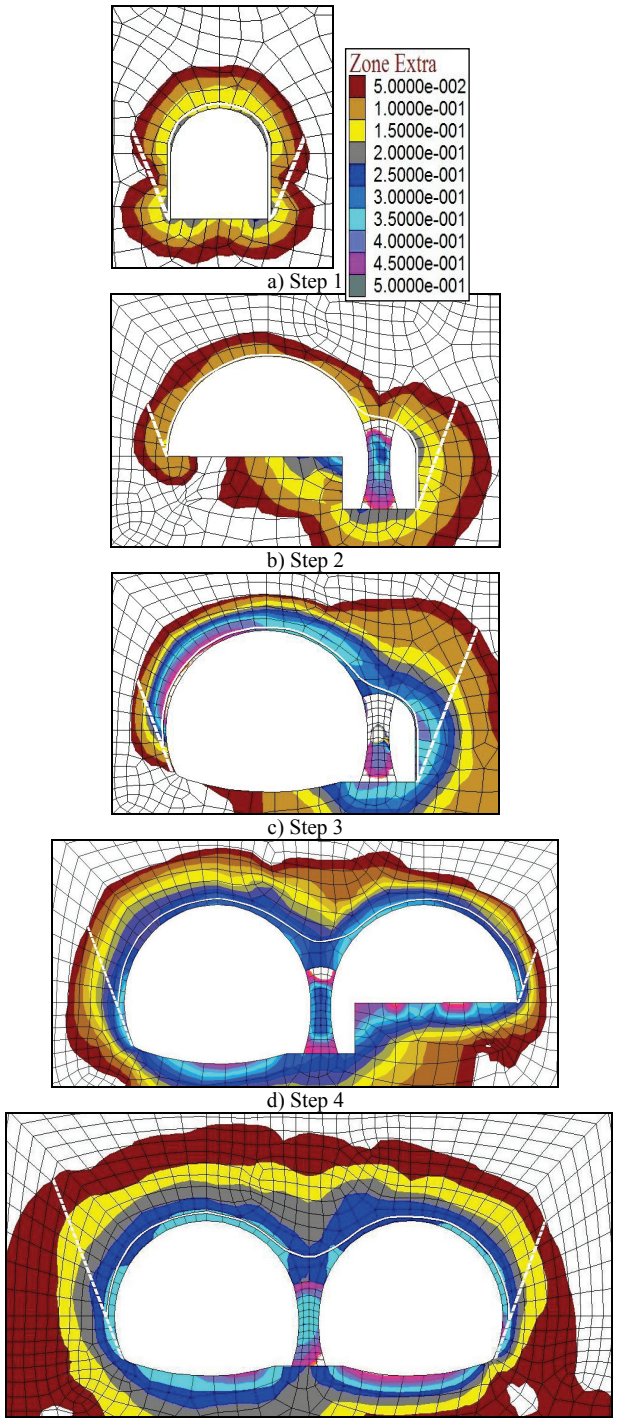

Figure 3 Pressure-arch evolution process under step-by-step excavation

Step 3: As shown in Fig. 3c, after the lower cross-section 3 of the left tunnel was excavated, the larger area of the surrounding rock was disturbed, the vault of zone 1 of the pressure-arch increased, and the thickness of zone 1

increased too; zone 2 of the pressure-arch started to develop to the left, the vault of zone 2 and the thickness of the pressure-arch increased obviously, and the stress concentration of the surrounding rock on the top of the middle pilot tunnel was significant, demonstrating the stress of the middle wall greatly increased.

Step 4: As shown in Fig. 3d, after the upper cross-section 4 of the right tunnel was excavated, the disturbance area of the surrounding rock was further enlarged, and the vault of zone 1 of the pressure-arch continued to increase, and the thickness of the pressure-arch further increased; zone 2 of the pressure-arch continued to develop to the left and the top, but its centre offset to zone 3 of the pressure-arch. At this time, zone 1, zone 2, and zone 3 of the pressure-arch generated newly were connected to form a skewed asymmetric combination pressure-arch.

Step 5: As shown in Fig. 3e, after the lower cross-section 5 of the right tunnel was excavated, with the vault lifting and the thickness of zone 3 increasing, the area of the pressure-arch continued to increase and adjust, and finally there was stress concentration in zone 2, and the area of zone 1 was significantly greater than that of zone 3 of the pressure-arch, which suggested the stress on the vault of the left tunnel of double-arch tunnel was higher than that of the right tunnel, namely the combination pressure-arch of the double-arch tunnel showed a skewed distribution.

As shown in Fig. 4, during step-by-step excavation of the bench method, the height and the thickness of the combination pressure-arch in double-arch tunnel showed a gradual growth trend. Overall, the pressure-arch height of zone 1 was the largest and its increasing rate was the fastest, the pressure-arch height and increasing rate of zone 3 were minimal, and the pressure-arch height and increasing rate of zone 2 were medium. The changes of these curves demonstrated that the combination pressure-arch of the double-arch tunnel was a skewed distribution.

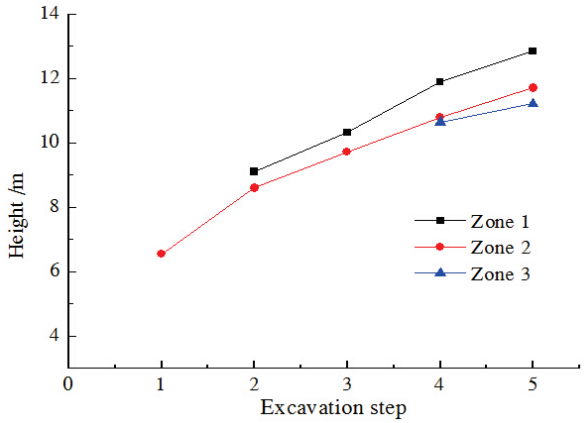

Figure 4 Vault height v S_1 ariation curves in different zones of the pressure-arch

4.2 Skewed effect analysis of the pressure-arch in the double-arch tunnel

The deformation of the tunnel can intuitively reflect the stress state of the surrounding rock, so during step-by-step excavation of the bench method, two displacement monitoring points P_1 and P_2 were set up respectively on the top of the middle wall of the double-arch tunnel as shown in Fig. 2a.

It can be seen from Fig. 5, the vertical displacements of points P_1 and P_2 were similar after the double-arch tunnel was excavated step-by-step, but there was an obvious difference between the horizontal displacements of points P_1 and P_2. After the excavation of the middle pilot tunnel, the points P_1 and P_2 respectively offset to the right and the left with a small horizontal displacement value; with the second and the third step excavation in the left tunnel, the horizontal displacements of points P_1 and P_2 offset to the left and both of the two points' displacement values showed a growth trend; after the fourth and fifth step excavation in the right tunnel, the horizontal displacement of P_2 began to offset to the right, but the horizontal displacement value was small, and however the horizontal displacement of P_1 had first a slight increase and then levelled off. Overall, the horizontal displacement of P_1 was greater than that of P_2.

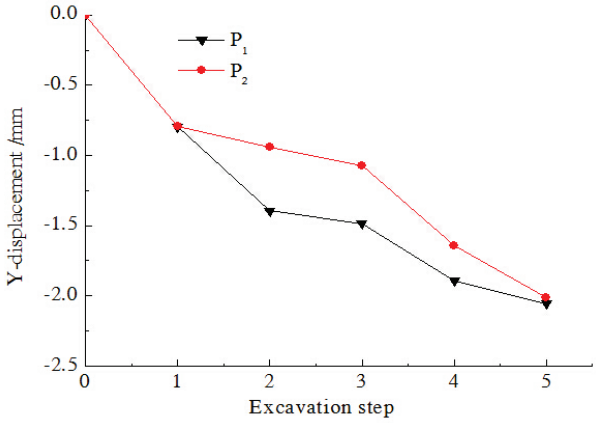

a) Vertical displacement curves

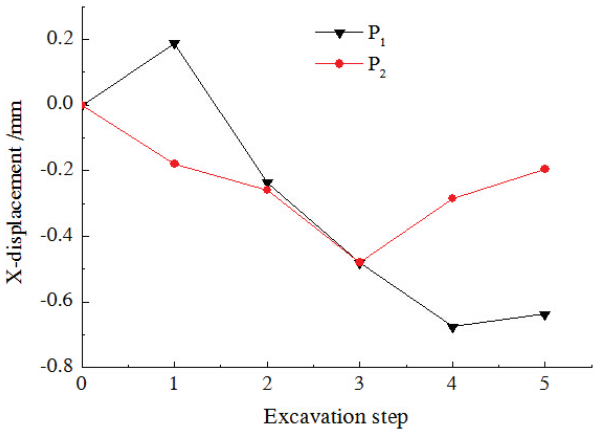

b) Horizontal displacement curves

Figure 5 Vertical and horizontal displacement curves of the monitoring points

To reflect the skewed effect of the surrounding rock stress of the double-arch tunnel, the skewed coefficient k was defined:

$$k = \left| \frac{d_{p1}}{d_{p2}} \right|, \tag{2}$$

where d_{p1} and d_{p2} are the horizontal displacement of points P_1 and P_2, respectively. If $k > 1$, the surrounding

rock deformation of the double-arch tunnel offsets to the left tunnel, which shows that the rock pressure of the double-arch tunnel is a skewed distribution to the left; if k = 1, the surrounding rock deformation of the left and the right sides is symmetrical, which suggests the rock pressure of the double-arch tunnel is a uniform distribution characteristic; if k < 1, the surrounding rock deformation offsets to the right tunnel, which suggests the rock pressure is a skewed distribution to the right. As shown in Fig. 6, during the step-by-step excavation of the bench method, the skewed coefficient k of the double-arch tunnel changed gradually from 1,0 to 3,5 showing the rock pressure skewed effect of the double-arch tunnel was significant, and the horizontal displacement of the middle wall of the double-arch tunnel mainly offset to the left tunnel.

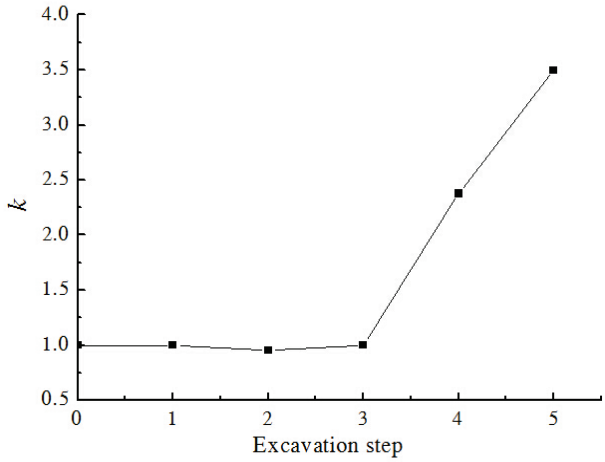

Figure 6 Skewed coefficient k variations of the double-arch tunnel

4.3 Strain energy entropy analysis of the pressure-arch evolution process

To reflect the energy dissipation characteristics of the pressure-arch and its stability in the evolution process of the double-arch tunnel, the concept of strain energy entropy was introduced. Assuming there was n unit body altogether in the excavation system of the double-arch tunnel, the strain energy of the i^{th} unit u_i is:

$$u_i = \int \frac{1}{2} \sigma_{ij} \varepsilon_{ij} \mathrm{d}v_i , \tag{3}$$

where σ_{ij} is the stress of unit, ε_{ij} is the strain of unit, v_i is the i^{th} unit volume, and the total strain energy U in the double-arch excavation system is:

$$U = \sum_{i=1}^{n} u_i . \tag{4}$$

Make

$$q_i = \frac{u_i}{U}, \tag{5}$$

and q_i meet $\sum_{i=1}^{n} q_i = 1$, $q_i \geq 0$ $(i = 1,2,\cdots,n)$, where q_i is the strain energy ratio of the i^{th} unit accounting for the total strain energy U.

The strain energy of the excavation system of the double-arch tunnel is converted to entropy, the strain energy entropy is S.

$$S = -\sum_{i=1}^{n} q_i \ln q_i \quad (i = 1,2,\cdots,n). \tag{6}$$

S was used to characterize the total strain energy distribution of the excavation system. The monitoring regions of strain energy entropy of the double-arch tunnel are shown in Fig. 7.

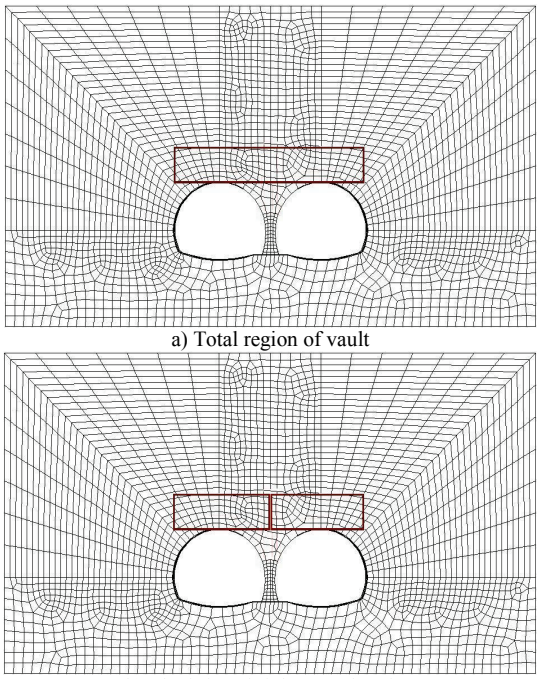

a) Total region of vault

b) The left and right tunnel region

Figure 7 Monitoring range of the strain energy entropy of the double-arch tunnel

As shown in Fig. 8a, during the step-by-step excavation of the bench method, the energy strain entropy curve on the roof of the double-arch tunnel appeared a ladder-like gradual declining trend. Along with the gradual release of the strain energy, the combination pressure-arch at the top of the double-arch tunnel tended to be gradually stable.

Fig. 8b showed that during the excavation process of the left tunnel and the right tunnel, the forming pressure-arches interacted, and the strain energy entropy curves on the left tunnel roof and the right tunnel roof both showed the overall downward trend, and the strain energy entropy value on the top of the left tunnel was greater than that of the right tunnel, which showed the pressure-arch stability of the right tunnel roof was better than that of the left tunnel, and therefore the rock bolting for the roof of the left tunnel in construction must be strengthened. The results showed that the evolution of the combination pressure-arch of the double-arch tunnel was a complex and gradually stable energy dissipation process in the excavation process.

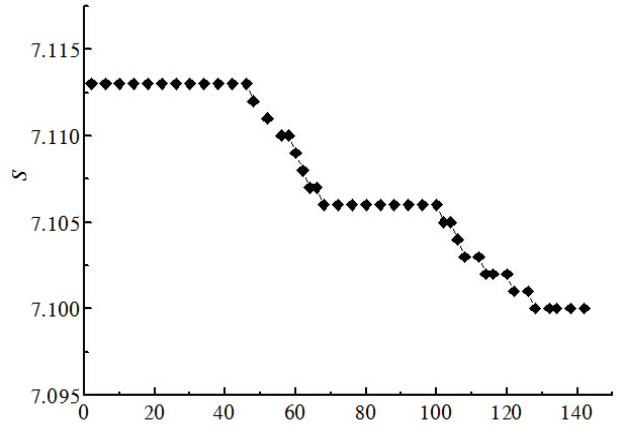

a) Total region of vault

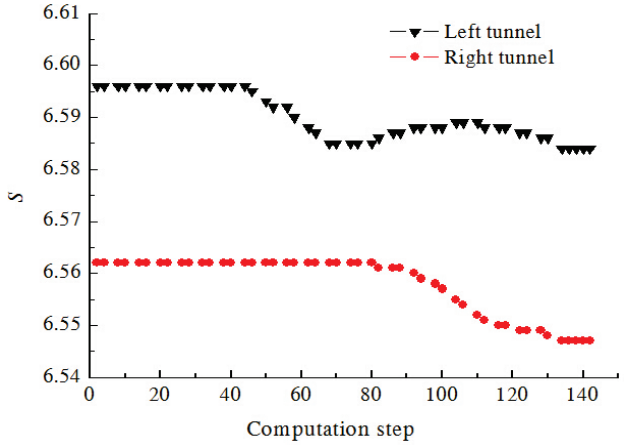

b) The left and right tunnel region

Figure 8 Monitoring curves of the strain energy entropy of the double-arch tunnel

5 Evolution characteristic analysis of the pressure-arch under different conditions

5.1 Geometric size effect

As shown in Figs. 9 and 10, under the same conditions, when the two-lane double-arch tunnels (the width of the right or the left tunnel is 12 m) and the three-lane ones (the width of the right or the left tunnel is 18 m) were excavated step-by-step by the bench method, it was found that the pressure-arches of the two-lane and three-lane tunnels displayed the skewed distribution characteristics. For the two-lane double-arch tunnel, the pressure-arch height in zone 1, zone 2 and zone 3 showed a gradual decreasing trend; and for the three-lane double-arch tunnel, the pressure-arch height in zone 1 and zone 2 were very close, and the pressure-arch height of zone 3 had a drastically reduced trend.

Seen from Fig. 11, during the step-by-step excavation, the skewed coefficient k of the pressure-arch of the two-lane double-arch tunnel changed gradually from 1,0 to 3,5, while that of the three-lane double-arch tunnel gradually increased from 1,0 to 8,0. Therefore, it could clearly be seen that with the increase of the tunnel span, the energy accumulation and release of the pressure-arch at the top of the pillar and the left tunnel were sensitive, and the skewed effect of the pressure-arch of the three-lane double-arch tunnel was much more significant than that of the two-lane one, which should be taken into consideration seriously in the supporting design and construction safety of the double-arch tunnel.

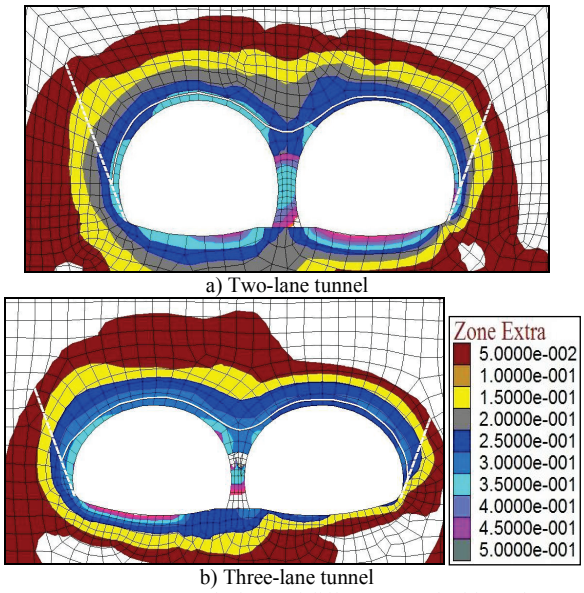

a) Two-lane tunnel

b) Three-lane tunnel

Figure 9 Pressure-arch shape of different span double-arch tunnel

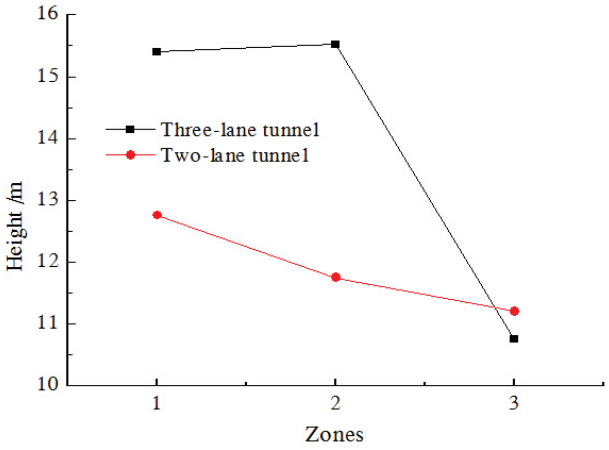

Figure 10 Vault height S_1 variations of different tunnels

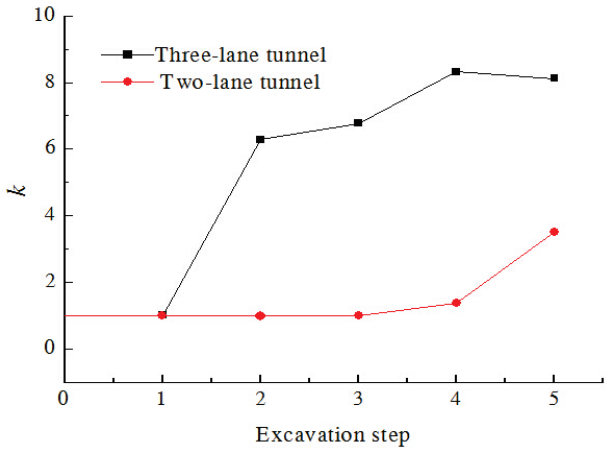

Figure 11 Skewed coefficient k variations of different tunnels

5.2 Construction sequence effect

As shown in Figs. 12 and 13, it was found that the pressure-arch height in zone 1 and zone 2 slightly increased after the double-arch tunnel was excavated by using the expand method, and the increasing rate of the

pressure-arch height in zone 3 was bigger, which made the pressure-arch distribution more uniform than that of the bench method, namely the skewed effect caused by step excavation of the expand method was relatively smaller than that of the bench method (See Fig.14).

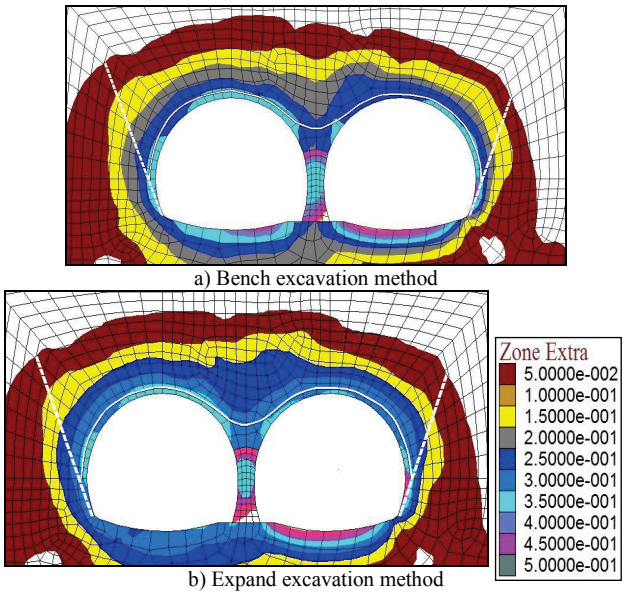

a) Bench excavation method

b) Expand excavation method

Figure 12 Pressure-arch shape of different excavation methods

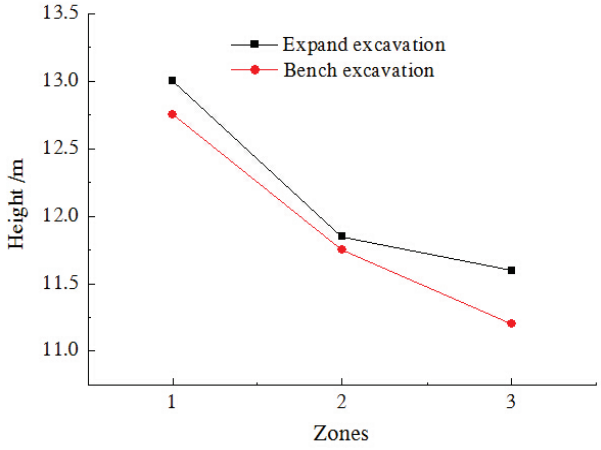

Figure 13 Vault height S_1 variations of different excavation

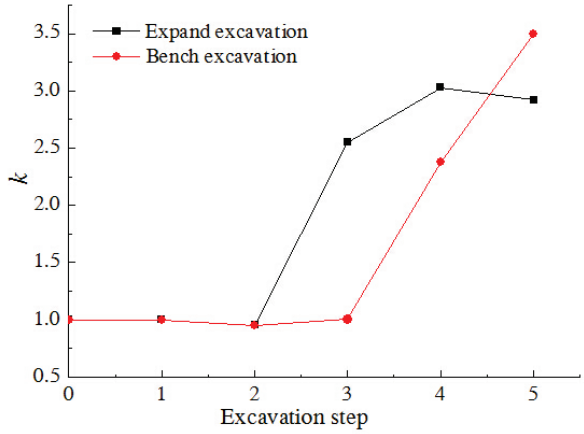

Figure 14 Skewed coefficient k variations of different

5.3 Stress state effect

As shown in Figs.15 and 16, with the change of the lateral pressure coefficient from high to low, the arch height of zone 1, zone 2 and zone 3 of the pressure-arch almost showed parting-step changed from high to low, the shape change of the pressure-arch was obvious. When λ was greater than 1, the arch heights of zone 1 and zone 3 of the pressure-arch showed a substantial upward bulge, and were significantly higher than that of zone 2; When λ was less than 1, relative to arch height of zone 1 of the pressure-arch, the arch heights of zone 2 and zone 3 of the pressure-arch drastically reduced; When λ equaled 1, relative to the above two cases, the arch height variation of the pressure-arch was between the above two cases, but in this stress state the arch height variation of the pressure-arch of the double-arch tunnel was smaller. Therefore, when λ was greater than 1 and when λ was less than 1, the influences on zone 1 and zone 3 of the pressure-arch of the double-arch tunnel were greater, the skewed distribution characteristics of the pressure-arch of the double-arch tunnel were obvious.

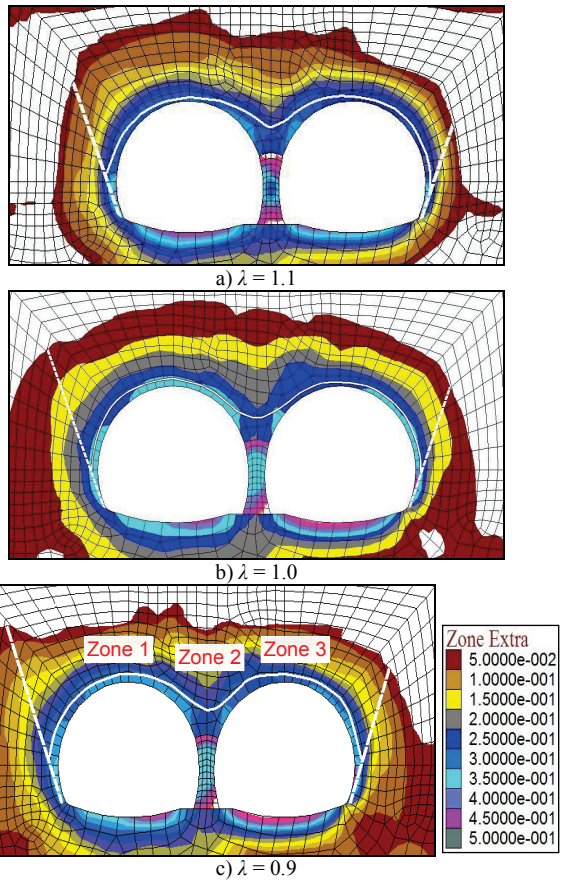

a) λ = 1.1

b) λ = 1.0

c) λ = 0.9

Figure 15 Pressure-arch shape under different stress states

As shown in Fig. 17, with the change of the lateral pressure coefficient of the tunnel surrounding rock from high to low, the skewed effect coefficient of the pressure-arch of the double-arch tunnel changed from 3,7; 3,5 to 8,9, therefore, when λ equaled 1, the skewed effect of the pressure-arch was relatively small, when λ was less than 1, the skewed effect of the pressure-arch was remarkable.

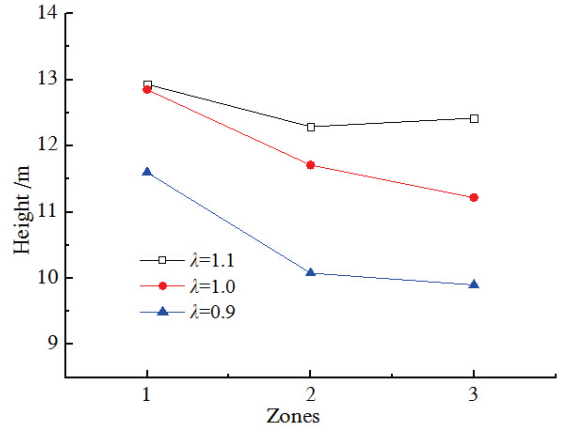

Figure 16 Vault height S_1 variations of different stress states

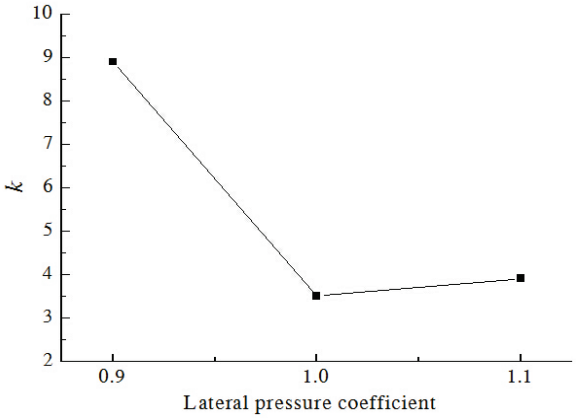

Figure 17 Skewed coefficient k variations of different

6 Conclusion

Along with the step-by-step excavation, the surrounding rock stress of the double-arch tunnel interacted, and then formed the complex pressure-arch. The arch height of the pressure-arch of the double-arch tunnel manifested the skewed distribution characteristics which were almost diminishing parting-step from the left tunnel to the right tunnel.

Based on the concepts of the skewed coefficient and the strain energy entropy, we can see that with the skewed effect of the pressure-arch the double-arch tunnel mainly offsets to the left tunnel, and that the strain energy dissipation characteristics of the double-arch tunnel are from high to low.

When the double-arch tunnel was excavated step-by-step, the obvious size effect of the pressure-arch was produced. The nonlinear response characteristics in different excavation sequences and the skewed effect with the change of the stress states were sensitive.

Acknowledgments

This work was financially supported by the National Natural Science Foundation of China (Nos. 51474188; 51074140; 51310105020), the Natural Science Foundation of Hebei Province of China (E2014203012), 2015 Endeavor Research Fellowship and Program for Taihang Scholars, all these are gratefully acknowledged.

7 References

[1] Wang, Y. Q.; Xie, Y. L. Research and development of multi-arch tunnel in China. // Highway. 6(2008), pp. 216-219.

[2] Majcherczyk, T.; Niedbalski, Z.; Małkowski, P.; Bednarek, Ł. Analysis of yielding steel arch support with rock bolts in mine roadways stability aspect. // Archives of Mining Sciences. 59, 3(2014), pp. 641-654. DOI: 10.2478/amsc-2014-0045

[3] Kovari, K. Erroneous concepts behind the New Austrian Tunneling Method. // Tunnels & Tunnelling International. 26, 11(1994), pp. 38-42.

[4] Bandis, S. C.; Lumsden, A. C.; Barton, N. R. Fundaments of rock joint deformation. // International Journal of Rock Mechanics and Mining Sciences & Geomechanics Abstracts. 20, 6(1983), pp. 249-268. DOI: 10.1016/0148-9062(83)90595-8

[5] Terzaghi, K. Evaluation of coefficient of subgrade reaction. // Geotechnique. 5, 4(1995), pp. 41-50.

[6] Muller, L.; Fecker, F. The elementary thought and primary principle of new Austrian tunneling method. // Underground Space. 6, (1980), pp. 26-32.

[7] Huang, Z. P.; Broch, E.; Lu, M. Cavern roof stability-mechanism of arching and stabilization by rock bolting. // Tunneling and Underground Space Technology. 17, 3(2002), pp. 249-261. DOI: 10.1016/S0886-7798(02)00010-X

[8] Poulsen, B. A.Coal pillar load calculation by pressure arch theory and near field extraction ratio. // International Journal of Rock Mechanics & Mining Sciences. 47, 7(2010), pp. 1158-1165. DOI: 10.1016/j.ijrmms.2010.06.011

[9] Fraldi, M.; Guarracino, F. Evaluation of impending collapse in circular tunnels by analytical and numerical approaches. // Tunneling and Underground Space Technology. 26, 4(2011), pp. 507-516. DOI: 10.1016/j.tust.2011.03.003

[10] Li, E. B.; Wang, D.; Wang, Y. Monitoring and control of construction deformation of urban shallow-buried large-span double-arch tunnel under complex condition. // Chinese Journal of Rock Mechanics and Engineering. 26, 4(2007), pp. 833-839.

[11] Zhu, Z. G.; Qiao, C. S.; Gao, B. B. Analysis of construction optimization and supporting structure under load of shallow multi-arch tunnel under unsymmetrical pressure. // Rock and Soil Mechanics. 29, 10(2008), pp. 2747-2752.

[12] Monjezi, M.; Rahmani, B. N.; Torabi, S. R.; Singh, T. N. Stability analysis of a shallow depth metro tunnel: a numerical approach. // Archives of Mining Sciences. 57, 3(2012), pp. 535-545. DOI: 10.2478/v10267-012-0035-0

[13] Ji, M. W.; Wu, S. C.; Gao, Y. T.; Ge, L. L.; Li, X. J. Construction monitoring and numerical simulation of multi-arch tunnel. // Rock and Soil Mechanics. 32, 12(2011), pp. 3787-3795.

[14] Yang, J. H.; Wang, S. R.; Wang, Y. G.; Li, C. L. Analysis of Arching Mechanism and Evolution Characteristics of tunnel pressure-arch. // Jordan Journal of Civil Engineering. 9, 1(2015), pp. 125-132.

[15] Chen, C. N.; Huang, W. Y.; Tseng, C. T. Stress redistribution and ground arch development during tunneling. // Tunneling and Underground Space Technology. 26, 1(2011), pp. 228-235. DOI: 10.1016/j.tust.2010.06.012

Authors' addresses

Shu-ren Wang, Ph.D., Professor, Corresponding author
Institution:
1) School of Civil Engineering and Mechanics, Yanshan University,
No. 438 Hebei West Street, Haigang District, Qinhuangdao,
066004, China
2) Opening Laboratory for Deep Mine Construction, Henan
Polytechnic University,
2001 Century Avenue, Jiaozuo, Henan Province, 454003, China
E-mail: w_sr88@163.com

Chun-liu Li, postgraduate
1) School of Civil Engineering and Mechanics, Yanshan University,
No. 438 Hebei West Street, Haigang District, Qinhuangdao,
066004, China
2) Institute of Urban Construction, Hebei Normal University of
Science & Technology, 066004, China
No. 360 Hebei West Street, Haigang District, Qinhuangdao,
066004, China
E-mail: lclcc_010@163.com

Yong-guang Wang, postgraduate
School of Civil Engineering and Mechanics, Yanshan University,
No. 438 Hebei West Street, Haigang District, Qinhuangdao,
066004, China
E-mail: lywangyongguang4@163.com

Zheng-sheng Zou, Ph.D., Professor, Corresponding author
Opening Laboratory for Deep Mine Construction, Henan
Polytechnic University,
2001 Century Avenue, Jiaozuo, Henan Province, 454003, China
E-mail: zouzs@hpu.edu.cn